PHYSICAL REVIEW B **84**, 201301(R) (2011)

Stress tuning of strong and weak couplings between quantum dots and cavity modes in microdisk microcavities

Hsuan Lin,[1] Chia-Hsien Lin,[1] Wei-Chen Lai,[1] Yi-Shan Lee,[2] Sheng-Di Lin,[2] and Wen-Hao Chang[1,*]

[1]*Department of Electrophysics, National Chiao Tung University, Hsinchu 300, Taiwan*

[2]*Department of Electronics Engineering, National Chiao Tung University, Hsinchu 300, Taiwan*

(Received 17 September 2011; published 1 November 2011)

We present the control of couplings between quantum dots and cavity modes in microdisk microcavities by a stress tuning scheme. The excitonic transitions and cavity modes can be brought into resonance due to their different energy shift rates with the applied strain. Spectral signatures of both strong and weak couplings are clearly observed. The strain tunable device can be used to tune the exciton wavelength bidirectionally at constant temperatures without significantly affecting the emission rate and linewidth of excitons.

DOI: 10.1103/PhysRevB.84.201301 PACS number(s): 78.67.Hc, 78.55.Cr

Cavity quantum electrodynamics (cQED) of systems with semiconductor quantum dots (QDs) coupled to the light confined in monolithic microcavities recently has been a research field of intense investigations. Such a solid-state cQED system offers a robust platform for exploring the fundamentals of light-matter interactions,[1–6] and also offers the basic building blocks for a variety of quantum information applications, such as single-photon sources,[7–9] entangled photon sources,[10] as well as quantum networks.[11,12] For most of these potential applications, strong coupling between an exciton and the cavity mode is an important prerequisite.[13] Recent progresses in the fabrication and design of microcavities with a high quality factor (Q) and a small mode volume have enabled the QD-based cQED systems to reach the strong coupling regime.[1–6] However, owing to the QD size fluctuation and the tolerance of cavity fabrication, postfabrication tunings of either the excitonic energy (E_X) or the cavity resonance (E_C) are usually inevitable. Furthermore, reversible fine tuning of the QD-cavity detuning ($\delta = E_X - E_C$) is also necessary in order to study the coupling behavior when an exciton and the cavity mode were brought into resonance. Strong coupling in various microcavities have been demonstrated by several tuning schemes, including varying the sample temperature,[1–3] depositing inert gases at low temperatures,[4,14] and applying an electric field[15] or a magnetic field.[16] The temperature tuning scheme is typically limited to the range of $T \lesssim 50$ K due to the quenching of QD emission and phonon-induced dephasing at elevated temperatures.[15,17] Similarly, the method based on inert gas condensation is applicable only at low temperatures.[4,14] The fine tuning by an electric field is very appealing in this regard, but the emission intensity and lifetime could be altered by the applied electric field due to the quantum-confined Stark effect.[18] The tuning of excitonic energy by a magnetic field falls into a special category for the study of spin-dependent coupling.[16] Another alternative is to apply an external stress,[19,20] which in principle has no temperature limit and less field-induced dephasing. However, to the best of our knowledge, strong coupling based on stress tuning has yet to be demonstrated.

In this Rapid Communication, stress tunings of the exciton energy in QDs embedded in microdisk (MD) microcavities are investigated. The strain distribution in the strain tunable device and the strain-induced energy shifts of the excitonic peaks and the cavity modes are analyzed. Spectral signatures in both the weak and strong coupling regimes are presented and discussed.

The sample was grown on a GaAs (001) substrate by molecular beam epitaxy. It consists of a 600-nm-thick $Al_{0.8}Ga_{0.2}As$ sacrificial layer on the substrate, followed by a 110-nm-thick GaAs waveguide layer with a layer of InAs self-assembled QDs embedded in the middle. The sample was processed into MDs by using electron-beam lithography. The waveguide layer and the sacrificial layer were etched in a HBr-based etchant. The sacrificial layer underneath the MDs was then completely removed in a buffered oxide etchant, leaving an array of MDs on the surface of the GaAs substrate.[21] The MDs were then transferred onto a piezoelectric actuator for applying stress at cryogenic temperature [see Fig. 1(a)]. The piezoelectric actuator is made of a 300-μm-thick $[Pb(Mg_{1/3}Nb_{2/3})O_3]_{0.72}$-$[PbTiO_3]_{0.28}$ (PMN-PT)[20,22] substrate coated with Ti/Au layers on the top and rear surfaces as electrodes. In order to provide optical confinements for MDs, a 500-nm-thick SiO_2 layer was further deposited on the top electrode. A layer of superglue (thickness ~400 nm) was spin coated on the SiO_2 surface. The GaAs substrate with MDs on the surface was subsequently upside down attached onto the superglue and baked at 100 °C for 3 min. After removing the substrate, the MDs were firmly glued on the SiO_2 layer. By applying a bias voltage (V_b) to the two electrodes to produce an out-of-plane electric field across the PMN-PT, an in-plane biaxial strain will be induced in the GaAs MDs as well as the embedded QDs.

Microphotoluminescence (μ-PL) measurements were carried out at $T \sim 6$ K by using a He-Ne laser as an excitation source. Emission signals were collected from the MD top and analyzed by a 0.75-m grating monochromator equipped with a liquid-nitrogen-cooled CCD camera, which yields a resolution-limited linewidth of ~60 μeV. Before optical measurements were taken, the PMN-PT was initially poled at $V_b = +300$ V during the cooling process so that an in-plane compressive (tensile) strain will be induced when $V_b > 0$ ($V_b < 0$) is applied.

Figure 1(b) shows the PL intensity map for a MD as a function of the emission wavelength and the applied V_b. Under low excitation conditions, all the PL lines shown here are excitonic emission lines from single QDs. When a positive (negative) bias voltage was applied to the PMN-PT,

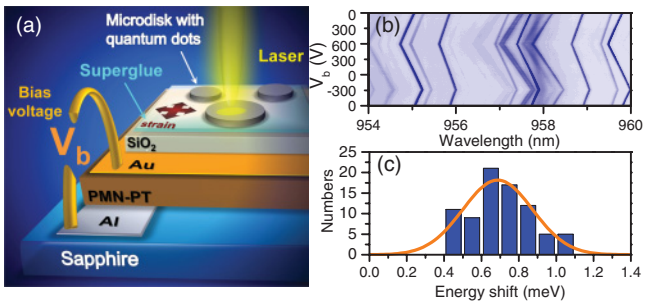

FIG. 1. (Color online) (a) Schematic drawing of the device used to apply in-plane biaxial strain to the GaAs microdisk microcavities with embedded InAs QDs. (b) Color-coded PL intensity map for a MD as a function of the emission wavelength and the bias voltage V_b applied to the PMN-PT. (c) A statistics of the total energy shift between $V_b = -300$ and $+600$ V for 80 QD emission lines from four different MDs.

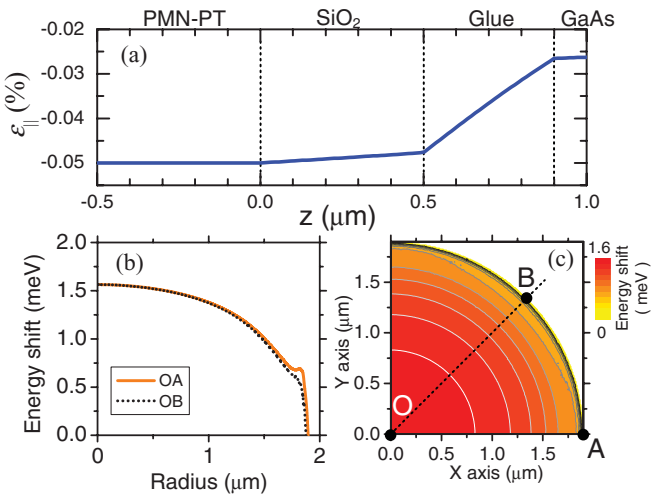

FIG. 2. (Color online) (a) The strain distribution along the vertical (z) direction of the device through the MD center calculated by FEM. (b) The radial distribution of the induced band-gap shift in the MD under an in-plane compressive strain of $\varepsilon_{\parallel} = -0.05\%$ at the SiO_2/PMN-PT interface. (c) A contour plot of the band-gap shift in the MD.

all the emission lines blueshift (redshift) linearly, but with an energy shift rate varying from line to line. A statistics of the total energy shift between $V_b = -300$ and $+600$ V for 80 emission lines from four different MDs is shown in Fig. 1(c). The distribution of the energy shift is widespread, with an average energy shift of $\sim$0.7 meV and a standard deviation of $\sim$0.4 meV. This corresponds to an average shift rate of $\sim$0.78 μeV/V. Since the energy shift is caused by the strain-induced band-gap shift, the widespread distribution suggests a nonuniform strain distribution in the MD.

To estimate the strain-induced energy shift in exciton lines, we need to know the in-plane strain produced by the PMN-PT. This can be estimated from the applied electric field F and the piezoelectric coefficient d_{31} of the $PMN_{0.72}$-$PT_{0.28}$ actuator. However, not much data has been reported for the piezoelectric properties of PMN-PT at low temperatures. Here we adopt the data reported in Herklotz *et al.*,[22] where the temperature evolution of the in-plane piezoelectric strain was measured from the macroscopic contraction of the sample length under an applied electric field. The in-plane strain at $T \leqslant 10$ K was found to be $\approx$0.05% under an applied field of $F = 30$ kV/cm, which is $\sim 1/4$ of its room-temperature value.

Having an idea about the in-plane strain produced in the PMN-PT, we then need to know how much of the strain has been delivered into the MDs through the SiO_2 and the glue layers. We have used the finite-element method (FEM) to simulate the strain distribution. Here the MD is considered as an isotropic material with a Young's modulus of 87 GPa and a Poisson's ratio of 0.31. The Young's modulus (Poisson's ratio) for the SiO_2 and the superglue layers are 70 GPa (0.17) and 7.5 GPa (0.35), respectively. Figure 2(a) shows the strain distribution along the vertical (z) direction of the device through the center of the MD. For an in-plane compressive strain of $\varepsilon_{\parallel} = -0.05\%$ in the PMN-PT, we found that only approximately half of the strain was delivered to the bottom of the GaAs MD. Most of the strain was lost in the glue layer because of its small Young's modulus. Reducing the thickness of the glue layer or using a stiffer material as a glue layer could further increase the strain delivered to the MDs.

After calculating the strain distribution, the band-gap shift in the GaAs and the InAs can be determined by the deformation potentials according to the band lineups in the model-solid theory.[23] The lateral distribution of the band-gap shift of the InAs QDs in the MD under a compressive strain of $\varepsilon_{\parallel} = -0.05\%$ at the SiO_2/PMN-PT interface is shown in Figs. 2(b) and 2(c). The band-gap shift is $\approx$1.6 meV at the disk center, but it decreases gradually to zero near the edge due to the strain relaxation via the free MD surface and sidewalls. For the spectra shown in Fig. 1(b), the laser excitation spot was positioned near the MD edge in order to excite both the QDs and the whispering gallery mode (WGM) traveling around the MD circumference. That is the reason why the measured energy shift rate is widespread and smaller than the calculated energy shift at the MD center.

Figures 3(a) and 3(c) show the PL spectra for a particular MD under a high ($P_{ex} = 100$ μW) and a low ($P_{ex} = 4\mu$W) excitation conditions, respectively. The corresponding PL intensity maps as a function of V_b are displayed in Figs. 3(b) and 3(d). Under high excitation conditions, the PL spectrum is dominated by the cavity emissions. These cavity modes are WGMs, which can be classified by the transverse-electric-field modes $TE_{\ell,m}$, with ℓ and m denoting the radial and the azimuthal mode numbers, respectively. Three-dimensional finite-difference time-domain (3D-FDTD) calculations have been performed in order to characterize the observed WGMs. We consider a 110-nm-thick GaAs MD with a diameter of 3.8 μm on top of a superglue layer and a SiO_2 layer. Our calculations suggested that the two cavity modes shown in Fig. 3(a) are $TE_{2,23}$ and $TE_{1,27}$ WGMs. From $V_b = -300$ to $+600$ V, the WGMs also shift with the applied V_b, but with a total energy shift of only $\sim$0.3 meV (shift rate $\sim$0.33 μeV/V), which is significantly smaller than those of QDs shown in Fig. 1(b).

The shift of the WGMs can be attributed to the strain-induced change in the MD size and the change in the index

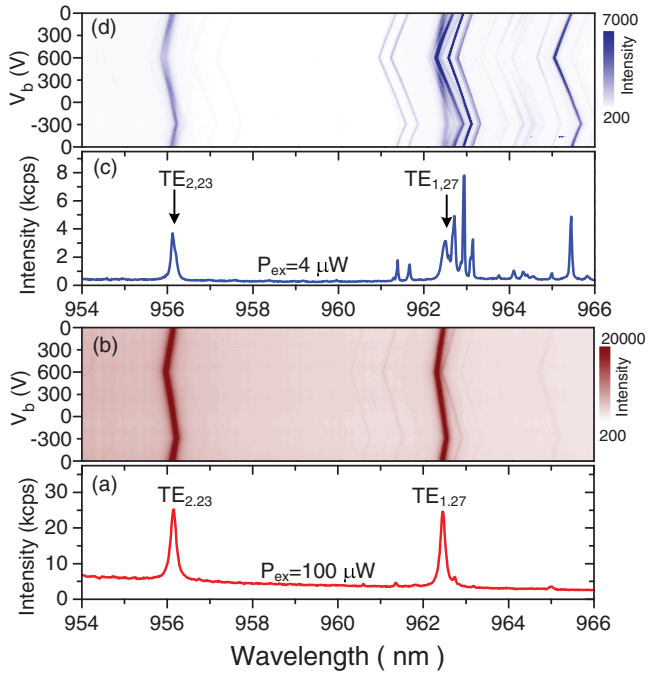

FIG. 3. (Color online) (a),(b) The PL spectrum taken at $V_b = 0$ V and the corresponding PL intensity map as a function of applied V_b for a particular MD at under a excitation power of $P_{ex} = 100\ \mu$W. (c),(d) The same as (a),(b) except that the excitation power was reduced to $P_{ex} = 4\ \mu$W.

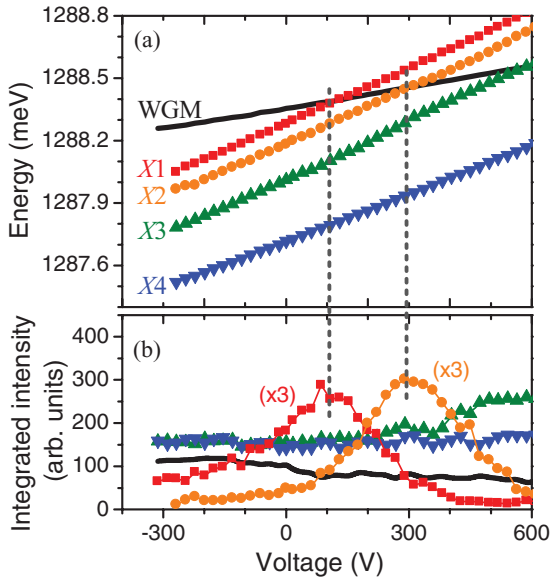

FIG. 4. (Color online) The peak energies (a) and the integrated intensities (b) as a function of V_b for four exciton lines ($X1$–$X4$) around the $TE_{1,27}$ WGM under a low excitation condition. Symbols and lines in (b) are the same as those in (a).

of refraction due to the photoelastic effect.[24] The shifts of WGMs with the MD diameter can be estimated from the 3D-FDTD calculations. For a compressive biaxial strain of $\varepsilon_{\parallel} = 0.026\%$ in the 3.8-μm MD, the diameter is contracted by ~1 nm, corresponding to a blueshift in $TE_{2,23}$ and the $TE_{1,27}$ WGMs by ~0.16 nm (0.22 meV), which is ~70% of the experimentally observed blueshift (0.3 meV). This indicates that the photoelastic effect is less important in the strain-induced WGM shifts.

Under a low excitation condition of $P_{ex} = 4\ \mu$W, both the cavity mode and the exciton lines of individual QDs can be resolved, as shown in Figs. 3(c) and 3(d). Since the exciton lines have larger strain-induced energy shifts, they can be brought into resonance with the WGMs by the applied stress. This can be seen from the emission lines near the $TE_{1,27}$ WGM at 962.5 nm, where the WGM shows crossings through different exciton lines at different V_b. To verify the QD-cavity coupling, we have extracted the peak energies and integrated intensities from the spectra by Lorentzian curve fittings, which are shown as a function of V_b in Figs. 4(a) and 4(b). With increasing V_b, the WGM crosses sequentially through exciton lines $X1$, $X2$, and $X3$. Around these crossing points, the PL intensities are enhanced by the cavity resonance. The peak crossings and the PL enhancements indicate that the QD-cavity couplings for these exciton lines are in the weak coupling regime.

In Fig. 5(a), the evolution of PL spectra near the $TE_{2,23}$ WGM with the applied V_b is displayed. The corresponding peak energies obtained by Lorentzian curve fittings are shown in Fig. 5(b). At $V_b = 0$, two emission peaks separated by ~0.1 nm can be resolved. According to the power-dependent measurements, we identified that the shorter wavelength peak is the $TE_{2,23}$ WGM (C), whereas the longer one is an exciton line (X) from a single QD. As X and C were brought into resonance by the applied V_b, the two peaks exhibit an anticrossing, indicative of strong coupling. The exact resonance can be examined by the energy splitting (ΔE) between the two peaks shown in Fig. 5(c), where the splitting goes through a minimum of $\Delta E = 88\ \mu$eV at $V_b = +162$ V.

The QD-cavity coupled system can be described by the Jaynes-Cummings Hamiltonian. After including damping

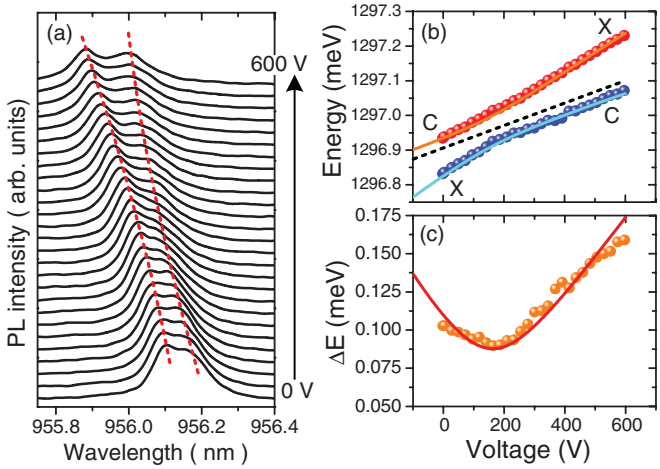

FIG. 5. (Color online) (a) The evolution of PL spectra near the $TE_{2,23}$ WGM with the applied bias voltage. The peak energies (b) and the energy splitting ΔE (c) as a function of the applied voltage V_b. The solid lines in (b),(c) are calculated from Eq. (1). The dotted line in (b) indicates the energy shift rate of the WGM obtained under high excitation conditions.

terms, the eigenstates are given by

$$E_{1,2} = \frac{E_X + E_C}{2} - i\frac{\gamma_X + \gamma_C}{4} \pm \sqrt{g^2 - \frac{(\gamma_C - \gamma_X - 2i\delta)^2}{16}}, \quad (1)$$

where $E_{X,C}$ and $\gamma_{X,C}$ are the energies and the linewidths of the exciton line (X) and the cavity mode (C), respectively; g represents the QD-cavity coupling strength and $\delta = E_X - E_C$ is the energy detuning. By considering the different energy shift rates of X and C in Eq. (1), the QD-cavity coupling strength was extracted to be $g = 51\mu$eV, corresponding to a coupling rate of 12.3 GHz.

The coupling strength for a QD placed at the antinode of the cavity field is given by[13] $g = \sqrt{\mu^2\hbar\omega/2\epsilon_0 n^2 V_m}$, where μ and ω are the dipole moment and the angular frequency of the exciton transition, and V_m is the effective modal volume of the cavity field. The excitonic dipole moment can be estimated from the spontaneous emission rate[13] $\gamma_{sp} = \mu^2\omega^3 n/3\pi\epsilon_0\hbar c^3$. For a measured $\gamma_{sp} \simeq 1.3\ \text{ns}^{-1}$ and a calculated $V_m \simeq 6(\lambda/n)^3$ for the WGM, the estimated coupling strength is $g \simeq 60\ \mu$eV. The measured g is very close to the ideal value, indicating that the misalignments of the dipole orientation and position with the cavity field are not apparent for the particular QD.

The stress tuning scheme is very appealing for the wavelength tuning of QD excitons at constant temperatures, particularly when a bidirectional tuning is necessary. An in-plane strain up to 0.1% could be attainable if the device design is further improved. In addition, we have also confirmed experimentally that the excitonic emission rate and linewidth (without the cavity effects) are nearly unchanged with the applied stress. However, we noted that the emission intensity was changed slightly due to the sample drift caused by the macroscopic contraction and expansion of the PMN-PT. This effect can be mitigated by placing the samples near the center of the device.

In summary, controlled couplings between quantum dots and cavity modes in microdisk microcavities by a stress tuning scheme are demonstrated. The exciton lines and cavity modes can be brought into resonance due to their different energy shift rates with the applied strain. Signatures of both strong and weak couplings are clearly resolved. The strain tunable device can be used to tune the exciton wavelength bidirectionally at a constant temperature without significantly affecting the emission rate and linewidth of excitons.

This work was supported in part by the program of MOE-ATU and the National Science Council of Taiwan under Grant No. NSC-99-2112-M-009-008-MY2.

*whchang@mail.nctu.edu.tw

[1] J. P. Reithmaier, G. Sek, A. Löffler, C. Hofmann, S. Kuhn, S. Reitzenstein, L. V. Keldysh, V. D. Kulakovskii, T. L. Reinecke, and A. Forchel, Nature (London) **432**, 197 (2004).

[2] T. Yoshie, A. Scherer, J. Hendrickson, G. Khitrova, H. M. Gibbs, G. Rupper, C. Ell, O. B. Shchekin, and D. G. Deppe, Nature (London) **432**, 200 (2004).

[3] E. Peter, P. Senellart, D. Martrou, A. Lemaître, J. Hours, J. M. Gérard, and J. Bloch, Phys. Rev. Lett. **95**, 067401 (2005).

[4] K. Srinivasan and O. Painter, Nature (London) **450**, 862 (2007).

[5] K. Hennessy, A. Badolato, M. Winger, D. Gerace, M. Atatüre, S. Gulde, S. Fält, E. L. Hu, and A. Imamoğlu, Nature (London) **445**, 896 (2007).

[6] D. Press, S. Götzinger, S. Reitzenstein, C. Hofmann, A. Löffler, M. Kamp, A. Forchel, and Y. Yamamoto, Phys. Rev. Lett. **98**, 117402 (2007).

[7] P. Michler, A. Kiraz, C. Becher, W. V. Schoenfeld, P. M. Petroff, L. Zhang, E. Hu, and A. Imamoğlu, Science **290**, 2282 (2000).

[8] C. Santori, M. Pelton, G. Solomon, Y. Dale, and Y. Yamamoto, Phys. Rev. Lett. **86**, 1502 (2001).

[9] W.-H. Chang, W.-Y. Chen, H.-S. Chang, T.-P. Hsieh, J.-I. Chyi, and T. M. Hsu, Phys. Rev. Lett. **96**, 117401 (2006).

[10] R. M. Stevenson, R. J. Young, P. Atkinson, K. Cooper, D. A. Ritchie, and A. J. Shields, Nature (London) **439**, 179 (2006).

[11] J. I. Cirac, P. Zoller, H. J. Kimble, and H. Mabuchi, Phys. Rev. Lett. **78**, 3221 (1997).

[12] W. Yao, R.-B. Liu, and L. J. Sham, Phys. Rev. Lett. **95**, 030504 (2005).

[13] G. Khitrova, H. M. Gibbs, M. Kira, S. W. Koch, and A. Scherer, Nat. Phys. **2**, 81 (2006).

[14] S. Mosor, J. Hendrickson, B. C. Richards, J. Sweet, G. Khitrova, H. M. Gibbs, T. Yoshie, A. Scherer, O. B. Shchekin, and D. G. Deppe, Appl. Phys. Lett. **87**, 141105 (2005).

[15] A. Laucht, N. Hauke, J. M. Villas-Bôas, F. Hofbauer, G. Böhm, M. Kaniber, and J. J. Finley, Phys. Rev. Lett. **103**, 087405 (2009).

[16] H. Kim, T. C. Shen, D. Sridharan, G. S. Solomon, and E. Waks, Appl. Phys. Lett. **98**, 091102 (2011).

[17] P. Borri, W. Langbein, U. Woggon, V. Stavarache, D. Reuter, and A. D. Wieck, Phys. Rev. B **71**, 115328 (2005).

[18] A. Laucht, F. Hofbauer, N. Hauke, J. Angele, S. Stobbe, M. Kaniber, G. Böhm, P. Lodahl, M.-C. Amann, and J. J. Finley, New J. Phys. **11**, 023034 (2009).

[19] S. Seidl, M. Kroner, A. Högele, K. Karrai, R. J. Warburton, A. Badolato, and P. M. Petroff, Appl. Phys. Lett. **88**, 203113 (2006).

[20] T. Zander, A. Herklotz, S. Kiravittaya, M. Benyoucef, F. Ding, P. Atkinson, S. Kumar, J. D. Plumhof, K. Dörr, A. Rastelli, and O. G. Schmidt, Opt. Express **17**, 22452 (2009).

[21] H. Lin, J.-H. Chen, S.-S. Chao, M.-C. Lo, S.-D. Lin, and W.-H. Chang, Opt. Express **18**, 23948 (2010).

[22] A. Herklotz, J. D. Plumhof, A. Rastelli, O. G. Schmidt, L. Schultz, and K. Dörr, J. Appl. Phys. **108**, 094101 (2010).

[23] C. G. Van de Walle, Phys. Rev. B **39**, 1871 (1989).

[24] C. W. Higginbotham, M. Cardona, and F. H. Pollak, Phys. Rev. **184**, 821 (1969).